

Molecular Assemblies of 4-(Hexadecyloxy)-*N*-(pyridinylmethylene)anilines at the Air–Water Interface and Cu(II)-Promoted Vesicle Formation via Metal Coordination

Haibo Wang,[†] Wangen Miao,^{*,‡} Huijin Liu,[†] Xianfeng Zhang,[†] and Xuezhong Du^{*,†}

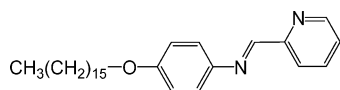
Key Laboratory of Mesoscopic Chemistry (Ministry of Education), State Key Laboratory of Coordination Chemistry, and School of Chemistry and Chemical Engineering, Nanjing University, Nanjing 210093, P. R. China, and School of Chemistry and Technology, Zhanjiang Normal University, Zhanjiang 524048, P. R. China

Received: June 27, 2010; Revised Manuscript Received: July 23, 2010

The molecular assemblies of 4-(hexadecyloxy)-*N*-(pyridinylmethylene)anilines (HPA) at the air–water interface on pure water and aqueous Cu(II) subphases have been investigated using in situ infrared reflection absorption spectroscopy (IRRAS). The Schiff base units were oriented with their long axes almost perpendicular to the water surface, and both imine and pyridinyl nitrogen atoms of the Schiff base units were coordinated to Cu(II) ions together with their geometrical conversions. The alkyl chains in the monolayers were quantitatively determined on the assumption that the HPA monolayers at the air–water interface were composed of sublayers of alkyl chains and Schiff base units, and the chain orientation angle on pure water was $30 \pm 2^\circ$ and increased to $37 \pm 2^\circ$ on the aqueous Cu(II) subphase. The HPA amphiphiles could not be dispersed in pure water but could self-organize into vesicles with metal-coordinated headgroups and interdigitated-packed alkyl chains in the presence of Cu(II) ions in aqueous solution. Transmission electron microscopy (TEM), differential scanning calorimetry (DSC), UV–vis spectroscopy, and small-angle X-ray diffraction (XRD) were used to investigate the aggregate structures and specific properties of the coordinated vesicles.

Introduction

Schiff bases and their metal complexes are one of the most important classes of organic compounds, with fascinating optical, electric, magnetic, and catalytic properties, and have extensive applications in photochromism/thermochromism,¹ liquid crystals,^{2,3} nonlinear optics,⁴ catalysis,⁵ and magnetic materials.⁶ However, their applications are restricted due to hydrolysis upon exposure to water. It has been shown that their stability and properties are greatly enhanced after the incorporation of Schiff base units into amphiphiles for effective self-assemblies of monolayers at the air–water interface⁷ and self-organization of bilayer membranes in aqueous solutions.⁸ A number of monolayers at the air–water interface^{10–17} and bilayer membranes in aqueous dispersions^{18–22} formed from the Schiff base derivatives have been reported, and hydrolysis was suppressed. Most of these studies are centered on the self-assembly and self-organization of Schiff base derivatives containing benzylidene and salicylidene moieties. In this paper, amphiphiles containing *N*-(pyridinylmethylene)aniline units, e.g., 4-(hexadecyloxy)-*N*-(pyridinylmethylene)aniline (HPA), were synthesized, and their monolayers at the air–water interface and Cu(II)-coordinated bilayer membranes in aqueous dispersions have been investigated in detail.



To date, Langmuir–Blodgett (LB) films of different kinds of Schiff base derivatives have been studied,^{12–17} but in situ

studies of their monolayers at the air–water interface are extremely limited.^{10,11} Infrared reflection absorption spectroscopy (IRRAS) has been a leading structural method for the in situ characterization of monolayers at the air–water interface.^{23–35} The IRRAS technique can not only allow for characterization of headgroup structures and chain conformations but can also provide quantitative information on molecular orientation. However, few of the monolayers composed of relatively complicated amphiphiles at the air–water interface have been studied using the IRRAS technique,^{10,11,36,37} particularly for the quantitative determination of molecular orientation.³⁸

Vesicles in aqueous solutions with a closed bilayer structure, similar to cell membranes predominantly consisting of phospholipids, have attracted great attention over the past three decades, ranging from fundamental areas in biochemistry and physical chemistry to many applicable aspects, such as pharmacology, catalysis, microreactor, and cosmetics.^{39,40} The design and construction of organized assemblies in aqueous solutions through noncovalent interactions, such as hydrogen bond, metal coordination, van der Waals force, and π – π stacking, have been extensively studied.^{18,39,40} The structures and properties of these aggregates are related not only to chemical structures of constituent molecules but also to surrounding environments, including pH, metal coordination, heat, light, etc.⁴¹ It is commonly considered that rigid conjugated segments (such as biphenyl, azobenzene, benzylideneaniline units, etc.) incorporated in alkyl chains are essential for single-chain amphiphiles (with charged headgroups) to strengthen hydrophobic interaction for the formation of stable bilayer membranes in aqueous solutions.^{18,39,40} Furthermore, Liang and co-workers proposed that the interactions between the hydrophilic headgroups through hydrogen bonds, electrostatic interaction, and metal coordination strengthened the interactions between the hydrophobic chains and induced a parallel chain arrangement to reach a new balance between the hydrophilic and hydrophobic interactions from a

* To whom correspondence should be addressed. E-mail: xzdu@nju.edu.cn; miaowangen@yahoo.com.cn; fax: 86-25-83317761.

[†] Nanjing University.

[‡] Zhanjiang Normal University.

series of studies of vesicle formation from single-chain amphiphiles without the rigid segment, monoalkylethylenediamine.^{42,43} In addition, vesicles can also be formed from some micelle-forming surfactants via metal coordination in aqueous solutions.^{44,45} However, the HPA amphiphiles could not be dispersed in pure water (pH 5.6) but could form stable monolayers at the air–water interface. In the presence of Cu(II) ions in aqueous solution, the amphiphiles could self-organize into vesicles with metal-coordinated headgroups and interdigitated-packed alkyl chains. Transmission electron microscopy (TEM), differential scanning calorimetry (DSC), UV–vis spectroscopy, and small-angle X-ray diffraction (XRD) were used to investigate the aggregate structures and specific properties of the formed vesicles.

Experimental Section

Materials. HPA was synthesized according to the method for the preparation of *N*-(4-dodecyloxysalicylidene)-4-aminobenzoic acid (DSA).¹⁰ ¹H NMR (Bruker DRX 500, CDCl₃): 8.7 (d, 1H, pyridinyl); 8.66 (s, 1H, CH=N); 8.2 (d, 1H, pyridinyl); 7.8 (m, 1H, pyridinyl); 7.3–7.4 (m, 2H, phenyl); 6.9 (d, 2H, phenyl); 4.0 (t, 2H, OCH₂); 1.8 (m, 2H, CH₂); 1.5 (m, 2H, CH₂); 1.3–1.4 (m, 24H, (CH₂)₁₂); 0.9 (t, 3H, CH₃). FTIR (Bruker VECTORTM 22, cm^{−1}): 2919 (ν_a (CH₂)); 2847 (ν_s (CH₂)); 1625 (ν (C=N)); 1579 (ν (C=C)); 1503 (ν (C=C)); 1464 (δ (CH₂)); 1244 (ν (=C–O)); 835 (ρ (=C–H)). 2-Pyridinecarbaldehyde was purchased from Alfa Aesar, and 1-bromohexadecane and 4-aminophenol were from Fluka. The chemical reagents used were of analytical grade, the water used was double distilled (pH 5.6) after a deionized exchange, and the aqueous CuCl₂ solution (1 mmol/L, pH 5.3) was not adjusted with acid or base.

Monolayer Spreading and Isotherm Measurements. Surface pressure–area (π –*A*) isotherms of HPA monolayers at the air–water interface were recorded on a Nima 611 Langmuir trough (Nima, England). A Wilhelmy plate (filter paper) was used as the surface pressure sensor and situated in the middle of the trough. Two barriers compressed or expanded symmetrically at the same velocity. Chloroform solutions of HPA (1 mmol/L) were spread on pure water and aqueous CuCl₂ subphases, and then 15 min was allowed for solvent evaporation. The two barriers compressed symmetrically at a rate of 5 mm/min. The subphase temperature was kept at 22 °C.

IRRAS Measurements. IRRAS spectra of the monolayers at the air–water interface were recorded on an Equinox 55 FTIR spectrometer (Bruker, Germany) connected to an XA-511 external reflection attachment with a shuttle trough system and a liquid-nitrogen-cooled MCT detector.^{36–38} Sample (monolayer-covered surface) and reference (monolayer-free surface) troughs were fixed on a shuttle device driven by a computer-controlled stepper motor for allowing collection from the two troughs in an alternating fashion. A KRS-5 polarizer was used to generate perpendicularly polarized beams, and the efficiency of the polarizer was determined to be about 99.1%. These spectral measurements were carried out at 22 °C. The HPA molecules were spread from a chloroform solution of desired volumes, and 15 min was allowed for solvent evaporation. The measurement system was then enclosed for humidity equilibrium and monolayer relaxation for 4 h prior to compression. The monolayers were compressed discontinuously to the desired surface pressure of 20 mN/m from ~0 mN/m. After 30 min of relaxation, the two moving barriers were stopped and the monolayer areas were kept constant. The external reflection absorption spectra of pure water and aqueous CuCl₂ solution

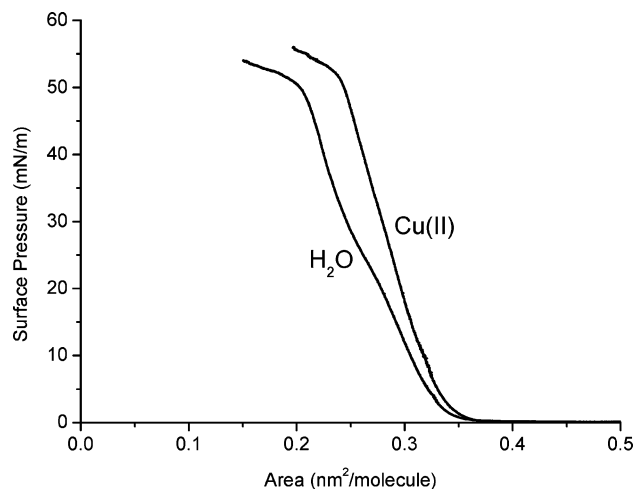


Figure 1. Surface pressure–area isotherms of the HPA monolayers on pure water and aqueous Cu(II) subphases at 22 °C.

were used as references, respectively. The spectra were recorded with a resolution of 8 cm^{−1} by coaddition of 1024 scans. A time delay of 30 s was allowed for film equilibrium between trough movement and data collection. Spectra were acquired using a p-polarized beam followed by data collection using an s-polarized beam. The IRRAS spectra were presented without smoothing or baseline correction.

Aqueous Dispersion in the Presence of Cu(II). After HPA was added to aqueous CuCl₂ solution, the system was first stirred for 10 h in order to wet the solid powder and then was ultrasonicated at 50 °C for 3 h followed by further ultrasonication in ice–water for 0.5 h to give a light yellow-red emulsion. The prepared emulsion (10 mmol/L) was stored at 4 °C, and dilute aqueous dispersions were prepared from the concentrated emulsion.

Instruments and Measurements. The dilute aqueous dispersion (0.9 mmol/L) was stained with 2 wt % aqueous uranyl acetate and then subjected to transmission electron microscope (JEM-200CX) measurement. DSC measurement was performed on a microcalorimeter (Pyris 1 DSC, PerkinElmer), and UV–vis spectra were recorded on a LAMBDA-35 spectrophotometer equipped with a variable-temperature attachment. The corresponding cast film was prepared by spreading a few drops of the aqueous dispersions on a glass plate followed by slow drying in a vacuum and then storage in a moist atmosphere for about 48 h at room temperature. The small-angle XRD patterns of the cast film were recorded on an X'Pert Pro X-ray diffractionmeter (Philips) with Cu–K α radiation (λ = 0.15418 nm).

Results and Discussion

Surface Pressure–Area (π –*A*) Isotherms. The geometrical structures of HPA amphiphiles were optimized by density functional theory calculation. The Schiff base units with imine and pyridinyl nitrogen atoms in *trans* positions were preferred in comparison to those in *cis* positions with a potential energy difference of 19.87 kJ/mol, and the *N*-phenyl planes were twisted from the *C*-pyridinyl planes at about 30° for the two geometries (Figure S1 in the Supporting Information). ¹³C NMR spectral studies indicated that the *N*-torsion angles for *trans*-*N*-(2-pyridylmethylene)anilines, the same Schiff base units as in HPA, were 34° in CDCl₃,⁴⁶ and their X-ray structural analysis showed that the *N*-phenyl planes in the crystal structure were twisted from the *C*-pyridinyl planes at angles of 20–35°. Figure 1 shows π –*A* isotherms of the monolayers of HPA at the

air–water interface on pure water and aqueous Cu(II) subphases, respectively. The amphiphiles formed a stable liquid-condensed monolayer on pure water with a small inflection around 25 mN/m, which probably resulted from a change in molecular orientation. The limiting areas of the monolayer on pure water were 0.33 and 0.28 nm² below and above the inflection, respectively, which was very close to the cross-sectional area perpendicular to the long axis of the Schiff base unit (0.27–0.28 nm²).¹² This suggests that the long axes of the Schiff base units were oriented almost perpendicular to the water surface. In the presence of Cu(II) ions, the monolayer was expanded to a certain extent, but the limiting area (0.33 nm²) remained unchanged in comparison with that on pure water below 20 mN/m. The metal complexes between the Schiff base units and Cu(II) ions probably gave rise to a tilt in orientation of the hydrocarbon chains.

IRRAS Spectra of Monolayers at the Air–Water Interface. It is well-known that IRRAS data are defined as plots of reflectance–absorbance (RA) versus wavenumber. RA is defined as $-\log(R/R_0)$, where R and R_0 are the reflectivities of the monolayer-covered and monolayer-free surfaces, respectively. In the case of s-polarization, the electric field vector is perpendicular to the plane of incidence, i.e., parallel to the water surface. The bands are always negative, and their intensities decrease with increasing angle of incidence.^{23,29,31} In the case of p-polarization, the electric field vector is parallel to the plane of incidence: (i) For the vibrations with transition moments parallel to the water surface, the bands are initially negative and their intensities increase with increasing angle of incidence and reach maximum values. Then minima in the reflectivity are found at the Brewster angle. Above the Brewster angle, the bands become positive, and their intensities decrease upon further increase of incidence angle.^{23,29,31} (ii) For the vibrations with their transition moments perpendicular to the water surface, the peaks are first positive and then become negative above the Brewster angle.^{23,31,32,48} (iii) If the vibrational transition moments are tilted to the air–water interface, the intensities of the bands are weak and even zero.⁴⁸

Figure 2 shows s-polarized IRRAS spectra of the monolayers of HPA on pure water and aqueous Cu(II) subphases at different surface pressures, respectively. On pure water, the two bands at 2918 and 2851 cm^{−1} at the surface pressure about 0 mN/m were due to the antisymmetric and symmetric CH₂ stretching vibrations ($\nu_a(\text{CH}_2)$ and $\nu_s(\text{CH}_2)$) of the hydrocarbon chains, respectively.^{49,50} It is known that the $\nu_a(\text{CH}_2)$ and $\nu_s(\text{CH}_2)$ frequencies are sensitive to the conformation order of alkyl chains.^{49,50} Lower wavenumbers are characteristic of preferential all-trans conformations in highly ordered chains, while the number of gauche conformers in disordered chains increases with the frequency and width of the bands.^{49,50} It is obvious that the hydrocarbon chains predominantly took ordered conformations in this case. The two bands increased in intensity but remained unchanged in frequency with the increase of surface pressure. The band at 1518 cm^{−1} was attributed to the skeleton stretching vibration of the aromatic rings ($\nu(\text{C}=\text{C})/\nu(\text{C}=\text{N})$).^{51–53} The band at 1468 cm^{−1} was due to the CH₂ scissoring mode [$\delta(\text{CH}_2)$],⁵⁴ indicative of a hexagonal subcell structure of the hydrocarbon chains.⁵⁵ The band at 1252 cm^{−1} was assigned to the =C–O stretching vibration ($\nu(\text{C}=\text{O})$) directly connected with the phenyl rings.^{11,51} On the aqueous Cu(II) subphase, the $\nu_a(\text{CH}_2)$, $\nu_s(\text{CH}_2)$, and $\delta(\text{CH}_2)$ bands remained constant in frequency but reduced in intensity due to increased molecular area and/or tilted chain orientation; however, the $\nu(\text{C}=\text{C})/\nu(\text{C}=\text{N})$ band shifted from 1518 to 1509 cm^{−1},

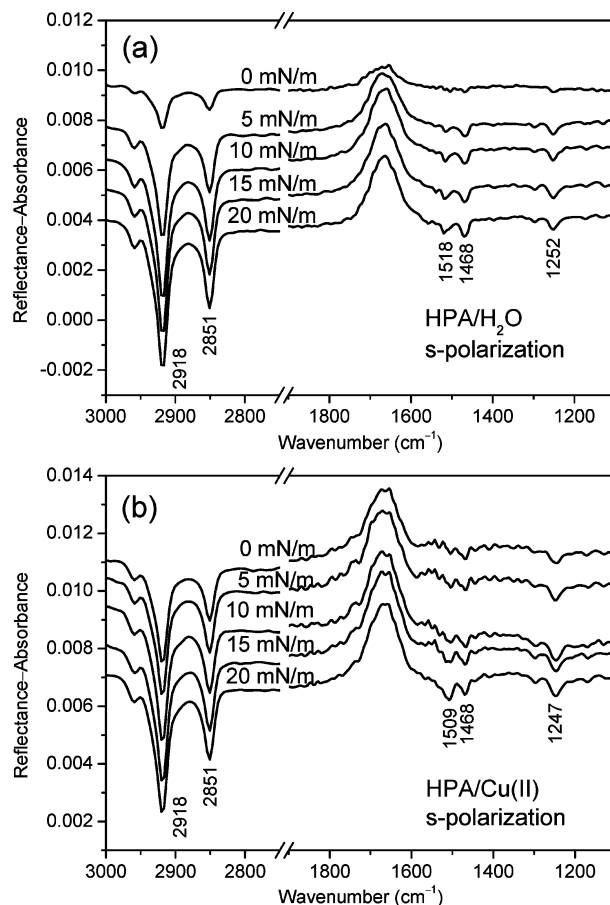


Figure 2. s-Polarized IRRAS spectra of the HPA monolayers with surface pressure at an angle of incidence of 30° at 22 °C: (a) pure water subphase; (b) aqueous Cu(II) subphase.

and the $\nu(\text{C}=\text{O})$ band from 1252 to 1247 cm^{−1}. The two decreased band frequencies indicated that the Cu(II) ions coordinated to both pyridinyl and imine nitrogen atoms of the Schiff base units. It is most likely that stable Cu(II) complexes of HPA were formed with the imine and pyridinyl nitrogen atoms in cis positions, converted from the initial trans positions. Fe(III) complexes of HPA and its analogues were reported recently,^{2,3} but their single crystals were not synthesized. The geometry optimizations of the Fe(III) complexes of HPA and its analogues were performed by computer simulation with the imine and pyridinyl nitrogen atoms in cis positions.^{2,3} Figure 3 compares p-polarized IRRAS spectra of the monolayers on pure water and aqueous Cu(II) solution at 20 mN/m below and above the Brewster angle, respectively. The $\nu_a(\text{CH}_2)$, $\nu_s(\text{CH}_2)$, and $\delta(\text{CH}_2)$ bands were negative below the Brewster angle (at the angle of incidence of 30°) and became positive above the Brewster angle (at the angle of incidence of 60°), which indicates that their vibrational transition moments were preferentially parallel to the water surface and that the alkyl chains were oriented far away from the water surface.^{23,29,31} Both the $\nu(\text{C}=\text{C})/\nu(\text{C}=\text{N})$ band around 1520–1500 cm^{−1} and the $\nu(\text{C}=\text{O})$ band were negative and weak below the Brewster angle and became more negative above the Brewster angle, which indicates that their vibrational transition moments were almost perpendicular to the water surface^{23,31,32,48} and that the long axes of the Schiff base units were oriented nearly perpendicular to the water surface, particularly for the monolayer on pure water.

For the two monolayers on the pure water and aqueous Cu(II) subphases at 20 mN/m (Figures S2 and S3 in the Supporting

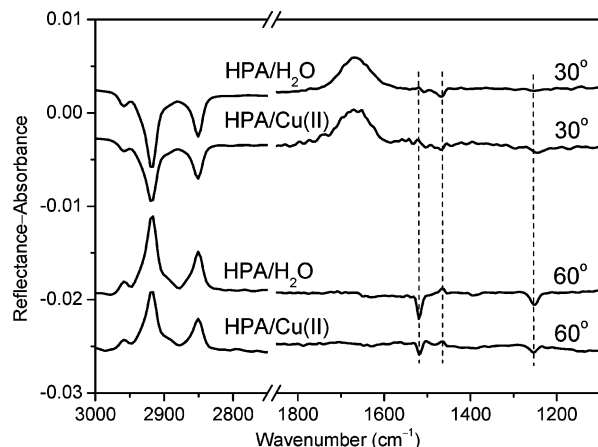


Figure 3. p-Polarized IRRAS spectra of the HPA monolayers on pure water and aqueous Cu(II) subphases at the surface pressure of 20 mN/m at 22 °C at the angles of incidence of 30 and 60° (below and above the Brewster angle), respectively.

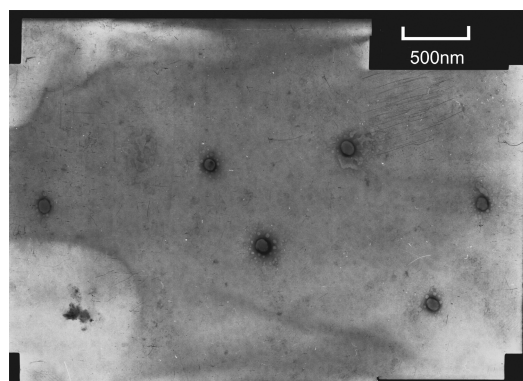


Figure 4. TEM image of the aggregates formed from the aqueous dispersion of HPA amphiphiles in the presence of Cu(II).

Information), their intensity ratios $\nu_a(\text{CH}_2)/\nu_s(\text{CH}_2)$ for p-polarization and s-polarization remained almost unchanged with angle of incidence (Figure S4 in the Supporting Information), which indicates that the ordered alkyl chains took a uniaxial orientation with free rotation of their CCC planes around their chain axes.^{23,33} Gericke et al. first applied the Kuzmin and Michailov optical model^{56,57} to describe IRRAS band intensities.^{23,24,28,29} Chain orientation angles can be determined by the simulation of theoretical calculations in the three-phase system (air, anisotropic monolayer, and isotropic aqueous subphase) to experimental data.^{24,28,29} Among the required parameters, film thickness (d) is important for the fit of theoretical calculations to experimental data. The method for the quantitative determination of chain orientation angles has been developed recently for the monolayers of relatively complicated amphiphiles such as DSA with a Schiff base unit on the assumption that the monolayer was composed of two sublayers of hydrocarbon chains and rigid Schiff base segments.³⁸ Similarly, the film thickness of the HPA monolayer was related to the tilt angle of the alkyl chains (θ_{chain}), extended lengths of chains (L_{chain}), and effective thickness of Schiff base segments (d_{sc}) by the relationship, $d = L_{\text{chain}} \cos \theta + d_{\text{sc}}$.³⁸ In the combination of the IRRAS results and π -A isotherms, the effective thickness of Schiff base segments could be roughly estimated. In the two HPA monolayers, the long axes of the Schiff base segments were nearly vertical to the water surface. The maximum extinction coefficient, k_{max} , is related to the extinction coefficient for the vibrational mode and density of the film-forming molecules at the air–water interface.³⁰ The

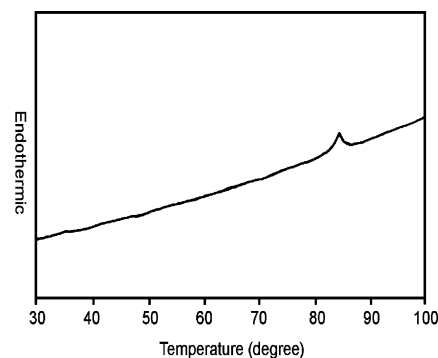


Figure 5. DSC curve of the aqueous dispersion of Cu(II)-coordinated HPA bilayer membranes.

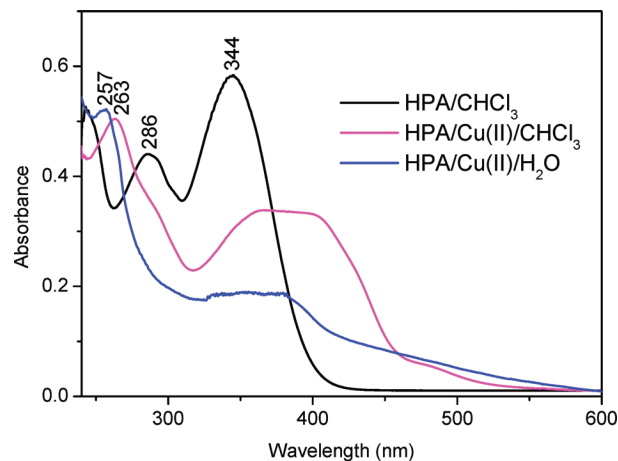


Figure 6. UV-vis spectra of the HPA amphiphiles and Cu(II)-coordinated HPA cast film in CHCl_3 and the aqueous dispersion of Cu(II)-coordinated HPA bilayer membranes.

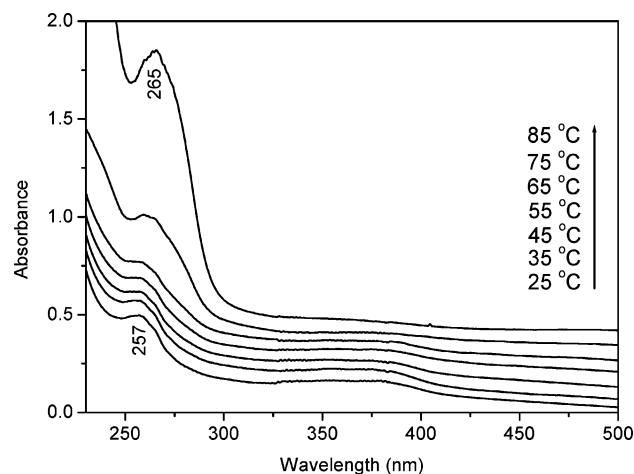


Figure 7. Temperature-dependent UV-vis spectra of Cu(II)-coordinated HPA bilayer membranes in aqueous solutions.

relative magnitude of the molecular density could be obtained from the appropriate π -A isotherms. The k_{max} value for the $\nu_a(\text{CH}_2)$ bands on the aqueous Cu(II) subphase was roughly estimated, taking into account the molecular area at 20 mN/m and the k_{max} value obtained on pure water. The simulated and measured RA values of the $\nu_a(\text{CH}_2)$ bands in the monolayers on the pure water and aqueous Cu(II) subphases against angle of incidence are shown in Figure S5 in the Supporting Information. The tilt angles of the alkyl chains were $30 \pm 2^\circ$ on pure water and $37 \pm 2^\circ$ on the aqueous Cu(II) subphase by the best fit.

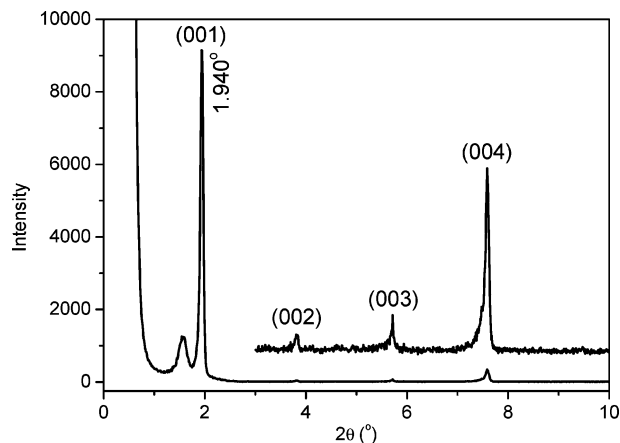


Figure 8. Small-angle XRD of the Cu(II)-coordinated HPA cast film.

Cu(II)-Coordinated Vesicles. HPA amphiphiles could not be dispersed in pure water (pH 5.6) but rather in aqueous Cu(II) solution in the form of a translucent emulsion. The aggregate morphologies of the HPA molecules in the presence of Cu(II) were observed by TEM (Figure 4). The almost spherical vesicles were formed with a mean size of about 150 nm. It is clear that the Cu(II) ions promoted the formation of vesicles via metal coordination.

Phase Transition of Bilayer Membranes. Phase transition is one of the basic physicochemical properties of bilayer membranes in aqueous dispersions.⁴⁰ An endothermic peak around 83.5 °C appeared, owing to the gel-to-liquid crystal phase transition in the DSC curve of the Cu(II)-promoted aqueous dispersion, and the corresponding enthalpy change was 42.4 kJ/mol (Figure 5). The enthalpy change was very comparable to those for most of aqueous dialkylammonium bilayers.¹⁸ Both

the high phase transition temperature and large enthalpy change indicate that the alkyl chains in the Cu(II)-coordinated bilayer membranes were most likely close-packed in an interdigitated type, taking the chemical structure of HPA into account.

UV–vis Spectra of Bilayer Membranes. The UV–vis spectra of HPA molecules and Cu(II)-coordinated HPA cast film in CHCl₃ are shown in Figure 6. In the case of HPA, two absorption maxima appeared at 286 and 344 nm. The maximum at 286 nm was ascribed to the π – π^* transition of a local excitation in the C₅H₄N–CH=N moieties, and the maximum at 344 nm was mainly assigned to the π – π^* charge transfer transition from the RO–C₆H₄ moieties to the C₅H₄N–CH=N moieties according to the spectral assignments of *N*-benzylideneanilines.⁵⁸ In general, the planarity of the *N*-benzylideneaniline derivatives is attributed to the favorable π -delocalization throughout the whole molecule by intramolecular charge transfer interaction between the substituents.⁵⁸ In the case of *N*-benzylideneanilines, the bands in the long wavelength region (band I) are expected to decrease in intensity with the increase of twist angle of nonplanar conformations, and on the contrary, the bands in the short wavelength region (band II) are expected to increase in intensity.⁵⁸ However, the planarization in each case is accompanied by an increase in the intensity of band I.^{8,20,58} For HPA in CHCl₃, the band at 344 nm was stronger than the band at 286 nm, which indicates that a great amount of planar conformations of the Schiff base units were preferred or that the twist angle between the *N*-phenyl and *C*-pyridinyl planes were not large. For the Cu(II)-coordinated HPA in CHCl₃, different spectral features were observed. The broad band around 400 nm was due to the ligand transition and a charge transfer from the Schiff base ligand to Cu(II), which confirms that the Cu(II) ions coordinated to the Schiff base units. The metal complex shows a strong shift to longer wavelength due to the greater degree of charge interactions between the Schiff base

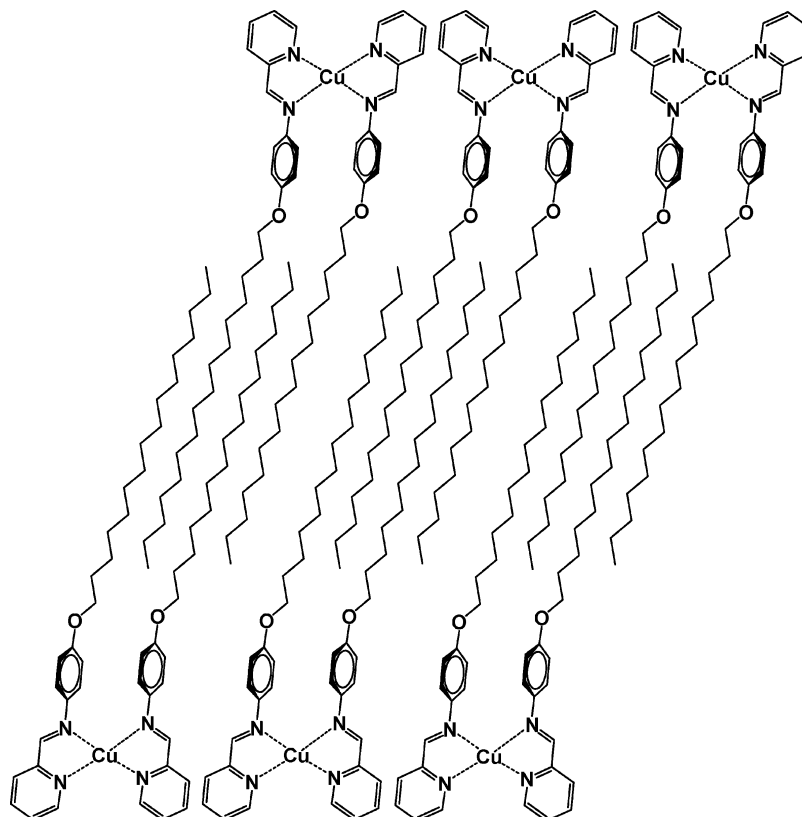


Figure 9. Schematic illustration of the Cu(II)-coordinated HPA bilayer membranes.

units and Cu(II) ions^{10,17,59} whereas for the Cu(II)-coordinated HPA in aqueous dispersion, the spectrum was similar to that in CHCl₃, with blue shifts of all bands, indicative of ordered stacking of the coordinated bilayers in water.

The variable-temperature UV–vis spectra of the coordinated bilayers in aqueous dispersion are shown in Figure 7. Below 65 °C, the spectra were the same as that at 25 °C, but when the temperature was elevated from 75 to 85 °C, the initial band at 257 nm was significantly intensified and shifted to 265 nm, close to the absorption maximum at 263 nm in CHCl₃. The temperature for the abrupt spectral change of the coordinated bilayers was in agreement with the phase transition temperature obtained from the DSC measurement, so the significant change of the band around 260 nm resulted from the gel–liquid crystal phase transition of the coordinated bilayers and not from the conformation change of the Schiff base units. However, the ligand-to-metal charge transfer absorption bands remained almost unchanged with temperature, which indicates that the band was insensitive to temperature change and that the metal coordination was existent even at elevated temperatures.

Small-Angle XRD of Cu(II)-Coordinated Cast Film. It has been established by many experiments that the self-organized structures of amphiphiles in dilute aqueous dispersions have been retained in moisture-saturated cast films under various conditions.^{42,60} Therefore, in order to determine the structural features of aqueous bilayer membranes, the small-angle XRD technique is usually used to study the long spacing of the cast bilayer membranes. There was one set of periodic diffraction peaks for the Cu(II)-coordinated cast film (Figure 8). According to the Bragg equation, the layer spacing was calculated to be 4.55 nm. Simultaneously, a weak and broad diffraction peak appeared, probably due to the formation of less ordered aggregates such as micelles in this case. From the DSC and variable-temperature UV–vis spectral results, only one gel–liquid crystal phase transition occurred. It is impossible that two types of bilayer membranes with different packing fashions were formed. Thus, interdigitated bilayer structures could be inferred from the layer spacing of 4.55 nm, taking into account the extended molecular length of HPA (3.25 nm) composed of a rigid Schiff base segment and an alkyl chain linked with an oxygen atom, which is schematically illustrated in Figure 9.

Conclusions

The HPA amphiphiles could form stable monolayers at the air–water interface on pure water and aqueous Cu(II) subphases. The in situ IRRAS spectral studies indicated that the long axes of the Schiff base units were oriented almost perpendicular to the water surface and that both imine and pyridinyl nitrogen atoms of the Schiff base units were coordinated to Cu(II) ions in addition to their geometrical conversion from trans to cis. The alkyl chains in the monolayers were quantitatively determined on the assumption that the HPA monolayers at the air–water interface were composed of sublayers of alkyl chains and Schiff base units by the fit of theoretical calculations to the spectral data. The alkyl chains were oriented at $30 \pm 2^\circ$ with respect to the normal of the monolayer on pure water and $37 \pm 2^\circ$ on the aqueous Cu(II) subphase. The HPA amphiphiles could not be dispersed in pure water but self-organized into vesicles with metal-coordinated headgroups in the presence of Cu(II) ions in aqueous solution. The high gel–liquid crystal phase transition temperature (83.5 °C), large enthalpy change (42.4 kcal/mol), and small layer spacing (4.55 nm in comparison with the extended molecular length of 3.25 nm) of the Cu(II)-coordinated bilayer membranes demonstrated that the alkyl

chains were packed in an interdigitated manner. The insoluble HPA amphiphiles could be converted into vesicles in aqueous solutions by metal coordination as well as into molecular assemblies of the monolayers at the air–water interface.

Acknowledgment. The work was supported by the National Natural Science Foundation of China (Grants 20873062) and the program for New Century Excellent Talents in University (NCET-07-0412).

Supporting Information Available: Geometrical optimization of HPA calculated by the B3LYP/6-31G(d) method (density functional theory), p- and s-polarized IRRAS spectra of the HPA monolayers on pure water and aqueous Cu(II) subphases at a surface pressure of 20 mN/m against different angles of incidence, intensity ratios of $\nu_a(\text{CH}_2)$ bands to $\nu_s(\text{CH}_2)$ bands, and simulation of theoretical calculations to spectral data for chain orientation angles. This information is available free of charge via the Internet at <http://pubs.acs.org>.

References and Notes

- (1) Hadjoudis, E.; Mavridis, I. M. *Chem. Soc. Rev.* **2004**, *33*, 579–588.
- (2) Hayami, S.; Danjobara, K.; Miyazaki, S.; Inoue, K.; Ogawa, Y.; Maeda, Y. *Polyhedron* **2005**, *24*, 2821–2827.
- (3) Hayami, S.; Motokawa, N.; Shuto, A.; Masuhara, N.; Someya, T.; Ogawa, Y.; Inoue, K.; Maeda, Y. *Inorg. Chem.* **2007**, *46*, 1789–1794.
- (4) Sliwa, M.; Létard, S.; Malfant, I.; Nierlich, M.; Lacroix, P. G.; Asahi, T.; Masuhara, H.; Yu, P.; Nakatani, K. *Chem. Mater.* **2005**, *17*, 4727–4735.
- (5) Volpe, M.; Hartnett, H.; Leeland, J. W.; Wills, K.; Ogunshun, M.; Duncombe, B. J.; Wilson, C.; Blake, A. J.; McMaster, J.; Love, J. B. *Inorg. Chem.* **2009**, *48*, 5195–5207.
- (6) Arnold, P. L.; Potter, N. A.; Magnani, N.; Apostolidis, C.; Griveau, J.-C.; Colineau, E.; Morgenstern, A.; Caciuffo, R.; Love, J. B. *Inorg. Chem.* **2010**, *49*, 5341–5343.
- (7) Nagel, J.; Oertel, U.; Friedel, P.; Komber, H.; Möbius, D. *Langmuir* **1997**, *13*, 4693–4698.
- (8) Liang, Y.; Wu, L.; Tian, Y.; Zhang, Z.; Chen, H. J. *Colloid Interface Sci.* **1996**, *178*, 703–713.
- (9) Pasc-Banu, A.; Sugisaki, C.; Gharsa, T.; Marty, J.-D.; Gascon, I.; Pozzi, G.; Quici, S.; Rico-Lattes, I.; Mingotaud, C. *Angew. Chem., Int. Ed.* **2004**, *43*, 6174–6177.
- (10) Liu, H.; Du, X.; Li, Y. J. *Phys. Chem. C* **2007**, *111*, 17025–17031.
- (11) Liu, H.; Zheng, H.; Miao, W.; Du, X. *Langmuir* **2009**, *25*, 2941–2948.
- (12) Kawamura, S.; Tsutsui, T.; Saito, S.; Murao, Y.; Kina, K. J. *Am. Chem. Soc.* **1988**, *110*, 509–511.
- (13) Chen, X.; Xue, Q.-B.; Yang, K.-Z.; Zhang, Q.-Z. *Langmuir* **1995**, *11*, 4082–4088.
- (14) Liu, M.; Xu, G.; Liu, Y.; Chen, Q. *Langmuir* **2001**, *17*, 427–431.
- (15) Jiao, T.; Liu, M. *Langmuir* **2006**, *22*, 5005–5012.
- (16) Jiao, T.; Zhang, G.; Liu, M. *J. Phys. Chem. B* **2007**, *111*, 3090–3097.
- (17) Hinda, S. S.; Shakya, R.; Rannulu, N. S.; Allard, M. M.; Heeg, M. J.; Radgers, M. T.; da Rocha, S. R. P.; Verani, C. N. *Inorg. Chem.* **2008**, *47*, 3119–3127.
- (18) Kunitake, T.; Okahata, Y.; Shimomura, M.; Yasunami, S.; Takarabe, K. J. *Am. Chem. Soc.* **1981**, *103*, 5401–5413.
- (19) Nishimi, T.; Ishikawa, Y.; Ando, R.; Kunitake, T. *Recl. Trav. Chim. Pays-Bas* **1994**, *113*, 201–208.
- (20) Wang, X.; Shen, Y.; Pan, Y.; Liang, Y. *Langmuir* **2001**, *17*, 3162–3167.
- (21) Wang, C.; Huang, J.; Tang, S.; Zhu, B. *Langmuir* **2001**, *17*, 6389–6392.
- (22) Wang, C.; Gao, Q.; Huang, J. *Langmuir* **2003**, *19*, 3757–3761.
- (23) Mendelsohn, R.; Braunder, J. W.; Gericke, A. *Annu. Rev. Phys. Chem.* **1995**, *46*, 305–334.
- (24) Gericke, A.; Michailov, V.; Hühnerfuss, H. *Vib. Spectrosc.* **1993**, *4*, 335–348.
- (25) Gericke, A.; Hühnerfuss, H. *J. Phys. Chem.* **1993**, *97*, 12899–12908.
- (26) Gericke, A.; Hühnerfuss, H. *Langmuir* **1995**, *11*, 225–230.
- (27) Simon-Kutscher, J.; Gericke, A.; Hühnerfuss, H. *Langmuir* **1996**, *12*, 1027–1034.
- (28) Flach, C. R.; Gericke, A.; Mendelsohn, R. *J. Phys. Chem. B* **1997**, *101*, 58–65.

- (29) Gericke, A.; Flach, C. R.; Mendelsohn, R. *Biophys. J.* **1997**, *73*, 492–499.
- (30) Bi, X.; Taneva, S.; Keough, K. M. W.; Mendelsohn, R.; Flach, C. R. *Biochemistry* **2001**, *40*, 13659–13669.
- (31) Ren, Y.; Kato, T. *Langmuir* **2002**, *18*, 6699–6705.
- (32) Du, X.; Miao, W.; Liang, Y. *J. Phys. Chem. B* **2005**, *109*, 7428–7434.
- (33) Wang, Y.; Du, X.; Guo, L.; Liu, H. *J. Chem. Phys.* **2006**, *124*, 134706.
- (34) Dyck, M.; Kerth, A.; Blume, A.; Lösche, M. *J. Phys. Chem. B* **2006**, *110*, 22152–22159.
- (35) Zheng, J.; Leblanc, R. M. Infrared Reflection Absorption Spectroscopy of Monolayers at the Air–Water Interface. In *Advanced Chemistry of Monolayers at Interfaces*; Imae, T., Ed.; Elsevier B. V.: Amsterdam, 2007; Chapter 10.
- (36) Miao, W.; Du, X.; Liang, Y. *J. Phys. Chem. B* **2003**, *107*, 13636–13642.
- (37) Wang, Y.; Du, X.; Miao, W.; Liang, Y. *J. Phys. Chem. B* **2006**, *110*, 4914–4923.
- (38) Liu, H.; Miao, W.; Du, X. *Langmuir* **2007**, *23*, 11034–11041.
- (39) Ringsdorf, H.; Schlarb, B.; Venzmer, J. *Angew. Chem., Int. Ed.* **1988**, *27*, 113–158.
- (40) Kunitake, T. *Angew. Chem., Int. Ed.* **1992**, *31*, 709–726.
- (41) Menger, F. M.; Yamasaki, Y. *J. Am. Chem. Soc.* **1993**, *115*, 3840–3841.
- (42) Lu, X.; Zhang, Z.; Liang, Y. *Langmuir* **1997**, *13*, 533–538.
- (43) Li, C.; Lu, X.; Liang, Y. *Langmuir* **2002**, *18*, 575–580.
- (44) Martinez, J. S.; Zhang, G. P.; Holt, P. D.; Jung, H.-T.; Carrano, C. J.; Haygood, M. G.; Butler, A. *Science* **2000**, *287*, 1245–1247.
- (45) Luo, X.; Wu, S.; Liang, Y. *Chem. Commun.* **2002**, 492–493.
- (46) Denecke, E.; Müller, K.; Bluhm, T. *Org. Magn. Reson.* **1982**, *18*, 68–70.
- (47) Wiebcke, M.; Mootz, D. *Acta Cryst., Sect. B: Struct. Crystallogr. Cryst. Chem.* **1982**, *38*, 2008–2013.
- (48) Wang, C.; Zheng, J.; Oliveira, O. N., Jr.; Leblanc, R. M. *J. Phys. Chem. C* **2007**, *111*, 7826–7833.
- (49) Snyder, R. G. *J. Chem. Phys.* **1967**, *47*, 1316–1360.
- (50) Kawai, T.; Umemura, J.; Takenaka, T.; Kodama, N.; Seki, S. *J. Colloid Interface Sci.* **1985**, *103*, 56–61.
- (51) Kutsumizu, S.; Kato, R.; Yamada, M.; Yano, S. *J. Phys. Chem. B* **1997**, *101*, 10666–10673.
- (52) Tao, Y.-T.; Lin, W.-L.; Hietpas, G. D.; Allara, D. L. *J. Phys. Chem. B* **1997**, *101*, 9732–9740.
- (53) Kawai, T.; Umemura, J.; Takenaka, T. *Langmuir* **1990**, *6*, 672–676.
- (54) Snyder, R. G. *J. Mol. Spectrosc.* **1961**, *7*, 116–144.
- (55) Kimura, F.; Umemura, J.; Takenaka, T. *Langmuir* **1986**, *2*, 96–101.
- (56) Kuzmin, V. L.; Michailov, A. V. *Opt. Spectrosc.* **1981**, *51*, 383–385.
- (57) Kuzmin, V. L.; Romanov, V. P.; Michailov, A. V. *Opt. Spectrosc.* **1992**, *73*, 1–26.
- (58) Akaba, R.; Tokumaru, K.; Konayashi, T. *Bull. Chem. Soc. Jpn.* **1980**, *53*, 1993–2001.
- (59) Hemakanthi, G.; Dhathathreyan, A.; Möbius, D. *Colloids Surf. A* **2002**, *198–200*, 443–452.
- (60) Ishikawa, Y.; Kunitake, T. *J. Am. Chem. Soc.* **1986**, *108*, 8300–8302.

JP1059352